



Efficient multiple gene knockout in *Colletotrichum higginsianum* via CRISPR/C as9 ribonucleoprotein and URA3 -based marker recycling

Katsuma Yonehara, Naoyoshi Kumakura, Takayuki Motoyama, Nobuaki Ishihama, Jean-félix Dallery, Richard O'Connell, Ken Shirasu

► To cite this version:

Katsuma Yonehara, Naoyoshi Kumakura, Takayuki Motoyama, Nobuaki Ishihama, Jean-félix Dallery, et al.. Efficient multiple gene knockout in *Colletotrichum higginsianum* via CRISPR/C as9 ribonucleoprotein and URA3 -based marker recycling. *Molecular Plant Pathology*, 2023, 10.1111/mpp.13378 . hal-04174238v2

HAL Id: hal-04174238

<https://hal.inrae.fr/hal-04174238v2>

Submitted on 31 Jul 2023

HAL is a multi-disciplinary open access archive for the deposit and dissemination of scientific research documents, whether they are published or not. The documents may come from teaching and research institutions in France or abroad, or from public or private research centers.



L'archive ouverte pluridisciplinaire **HAL**, est destinée au dépôt et à la diffusion de documents scientifiques de niveau recherche, publiés ou non, émanant des établissements d'enseignement et de recherche français ou étrangers, des laboratoires publics ou privés.



Distributed under a Creative Commons Attribution - NonCommercial - NoDerivatives 4.0 International License

TECHNICAL ADVANCE

Efficient multiple gene knockout in *Colletotrichum higginsianum* via CRISPR/Cas9 ribonucleoprotein and *URA3*-based marker recycling

Katsuma Yonehara^{1,2}  | Naoyoshi Kumakura¹  | Takayuki Motoyama¹  |
Nobuaki Ishihama¹  | Jean-Félix Dallery³  | Richard O'Connell³  | Ken Shirasu^{1,2} 

¹RIKEN Center for Sustainable Resource Science, Yokohama, Japan

²Department of Biological Science, Graduate School of Science, The University of Tokyo, Tokyo, Japan

³Université Paris-Saclay, INRAE, UR BIOGER, Palaiseau, France

Correspondence

Ken Shirasu, RIKEN Center for Sustainable Resource Science, Tsurumi-ku, Yokohama 230-0045, Japan.

Email: ken.shirasu@riken.jp

Funding information

Japan Science and Technology Agency, Grant/Award Number: JPMJAX20B4; Japan Society for the Promotion of Science, Grant/Award Number: 19KK0397, 23K05158, JP18K14440, JP20H05909, JP20K15500 and JP22H00364

Abstract

Colletotrichum higginsianum is a hemibiotrophic pathogen that causes anthracnose disease on crucifer hosts, including *Arabidopsis thaliana*. Despite the availability of genomic and transcriptomic information and the ability to transform both organisms, identifying *C. higginsianum* genes involved in virulence has been challenging due to recalcitrance to gene targeting and redundancy of virulence factors. To overcome these obstacles, we developed an efficient method for multiple gene disruption in *C. higginsianum* by combining CRISPR/Cas9 and a *URA3*-based marker recycling system. Our method significantly increased the efficiency of gene knockout via homologous recombination by introducing genomic DNA double-strand breaks. We demonstrated the applicability of the *URA3*-based marker recycling system for multiple gene targeting in the same strain. Using our technology, we successfully targeted two melanin biosynthesis genes, *SCD1* and *PKS1*, which resulted in deficiency in melanization and loss of pathogenicity in the mutants. Our findings demonstrate the effectiveness of our methods in analysing virulence factors in *C. higginsianum*, thus accelerating research on plant–fungus interactions.

KEYWORDS

Arabidopsis thaliana, *Colletotrichum higginsianum*, CRISPR/Cas9, plant-pathogenic fungus, selection marker recycling, *URA3*

1 | INTRODUCTION

Phytopathogenic fungi cause significant crop losses annually, leading to serious economic losses (Fisher et al., 2012; Oerke, 2006). Among them, *Colletotrichum* spp. are in the top 10 most economically and scientifically important phytopathogenic fungi, due to their wide host range and hemibiotrophic lifestyle (Dean et al., 2012). Members of the genus *Colletotrichum* are responsible for anthracnose disease

in thousands of plant species and undergo, in general, two distinct phases during the infection process, namely, the biotrophic and necrotrophic phases (Cannon et al., 2012; Münch et al., 2008; Perfect et al., 1999). Infection begins with the development of melanized appressoria from fungal spores, which generate a high turgor pressure to penetrate the host plant's cuticle and cell wall. In the subsequent biotrophic phase, the fungi extend their mycelia within the living host cells to obtain nutrients. Infection is completed

This is an open access article under the terms of the [Creative Commons Attribution-NonCommercial-NoDerivs](https://creativecommons.org/licenses/by-nc-nd/4.0/) License, which permits use and distribution in any medium, provided the original work is properly cited, the use is non-commercial and no modifications or adaptations are made.

© 2023 The Authors. *Molecular Plant Pathology* published by British Society for Plant Pathology and John Wiley & Sons Ltd.

in the necrotrophic phase, marked by host cell death and the formation of spores (Cannon et al., 2012). This dynamic lifestyle transition makes *Colletotrichum* spp. valuable subjects for research on plant–fungus interactions.

Within the genus, *Colletotrichum higginsianum* is a suitable model for exploring plant–fungus interactions due to its ability to infect cruciferous plants, including *Arabidopsis thaliana*, a species with extensive genomic and transcriptomic resources and genetic tools (Narusaka et al., 2004; O'Connell et al., 2004). Studies involving genetic crosses of ecotypes with varying resistance to *C. higginsianum* have led to the identification of resistance genes in *A. thaliana* (Birker et al., 2009; Narusaka et al., 2009). On the fungal side, genomic and transcriptomic analyses of *C. higginsianum* have highlighted the potential contribution of secondary metabolites and secreted proteins to infection (Dallery et al., 2017; Kleemann et al., 2012; O'Connell et al., 2012; Tsushima et al., 2019; Tsushima & Shirasu, 2022). For instance, the secondary metabolite higginsianin B and extracellular LysM proteins of *C. higginsianum* have been found to suppress plant immune responses (Dallery et al., 2020; Takahara et al., 2016). Further, targeted gene disruption is possible in *C. higginsianum* through *Agrobacterium tumefaciens*-mediated or polyethylene glycol (PEG)-mediated protoplast transformation, allowing the search for pathogenicity genes (Huser et al., 2009; Ushimaru et al., 2010), and homologous recombination using donor DNA enables disruption of target genes. However, the molecular mechanisms underlying the infection of *C. higginsianum* are not yet fully understood, probably due to the recalcitrance of some genes to manipulation (Huser et al., 2009; Ushimaru et al., 2010) and the redundancy of pathogenicity genes (Collemare et al., 2019; Kleemann et al., 2008). Therefore, the development of high-efficiency multiple gene disruption in *C. higginsianum* would be valuable for uncovering plant–fungus interactions, but such technology is currently unavailable for this species.

The clustered regularly interspaced short palindromic repeats (CRISPR)/CRISPR-associated protein 9 (Cas9) system is a revolutionary tool for genome editing, increasing the efficiency of gene disruption via homologous recombination in various organisms. It operates by inducing double-strand breaks (DSBs) in genomic DNA (Belhaj et al., 2015; Sander & Joung, 2014; Schuster & Kahmann, 2019) using ribonucleoproteins (RNPs) comprising Cas9 proteins and guide RNAs (gRNAs) that target specific sequences. The resulting repair of DSBs through nonhomologous end joining (NHEJ) or homology-directed repair (HDR) pathways (Capecchi, 1989; Pastink et al., 2001) enables targeted gene manipulation. Artificially inducing DSBs in target regions with CRISPR/Cas9 significantly increases the efficiency of homologous recombination using donor DNA (Devkota, 2018; Gratz et al., 2014). This technique has been demonstrated and used in several phytopathogenic fungi, including *Magnaporthe oryzae* (Arazoe et al., 2015; Foster et al., 2018), *Botrytis cinerea* (Leisen et al., 2020), *Penicillium expansum* (Clemmensen et al., 2022), *Colletotrichum sansevieriae* (Nakamura et al., 2019), and *Colletotrichum orbiculare* (Chen et al., 2023; Yamada et al., 2023). Nevertheless, despite its effectiveness, CRISPR/Cas9 has not yet been applied to *C. higginsianum*.

A selection marker recycling system in combination with homologous recombination has enabled the efficient disruption of multiple genes in a variety of fungi. The *URA3*-based marker recycling system that relies on the versatile *URA3* gene, encoding orotidine-5' phosphate decarboxylase involved in uridine synthesis (Weld et al., 2006), has been widely used in fungi, such as yeast (Alani et al., 1987), *Aspergillus* (d'Enfert, 1996; Nielsen et al., 2006; Oakley et al., 1987), and *C. orbiculare* (Kumakura et al., 2019). In this system, using *ura3* mutants exhibiting uridine/uracil auxotrophy as recipients, strains can be selected in which the target loci in the genome are replaced with donor DNA containing a *URA3* expression cassette on selection media without uridine/uracil. Negative selection can then be used to select for strains that lost the *URA3* cassette using 5-fluoroorotic acid (5-FOA), a uridine precursor analogue, because 5-FOA is converted into the toxic compound fluorouracil by *URA3* (Boeke et al., 1984; Flynn & Reece, 1999). The *URA3* cassette can be removed from the genome via homologous recombination if it is flanked by any two homologous sequences, which do not have to be specific sequences such as *hisG* repeats used previously (Alani et al., 1987). This selection system can be repeated as many times as necessary to achieve multiple gene disruption with one selection marker. The *URA3*-based marker recycling system should be applicable to *C. higginsianum*, as fungi generally possess the *URA3* gene.

Here, we report the establishment of an efficient multiple gene disruption method in *C. higginsianum* combining CRISPR/Cas9 and *URA3*-based marker recycling. By using in vitro formed CRISPR/Cas9 RNPs in the PEG-mediated transformation of *C. higginsianum* protoplasts with donor DNA, we observed a significant increase in gene knockout efficiency. Using *URA3*-based marker recycling, we demonstrated the capacity for multiple gene disruption in the same strain by sequentially targeting two melanin biosynthesis genes, *SCD1* and *PKS1*. The *scd1* and *pkd1 scd1* mutants exhibited melanin deficiency and loss of pathogenicity on *A. thaliana* leaves, demonstrating the effectiveness of this method for phenotypic analysis of virulence-related genes. Our results establish a highly efficient multiple gene disruption method in *C. higginsianum*, which has the potential to aid the identification of previously unidentified virulence factors.

2 | RESULTS

2.1 | CRISPR/Cas9 RNP enhances the rate of donor DNA-mediated homologous recombination in *C. higginsianum*

To identify the *URA3* homologue in the *C. higginsianum* genome, we employed the NCBI BlastP tool with default settings and used *S. cerevisiae* *URA3p* (GenBank ID: NP_010893.3) as the query sequence. As previously reported (Kumakura et al., 2019), *URA3* homologues are generally well conserved among phytopathogenic fungi. Accordingly, we identified one *URA3* homologue in the *C. higginsianum* genome (locus tag: CH63R_12904; Figure S1). We attempted



to disrupt *URA3* using PEG-mediated protoplast transformation. However, *ura3* mutants were rarely obtained (Table 1), probably due to the low frequency of DSBs. Therefore, we introduced CRISPR/Cas9 technology to induce DSBs and promote homologous recombination with donor DNA. The transformation method with CRISPR/Cas9 RNP consists of three steps (Figure 1a). First, Cas9 recombinant proteins and synthetic gRNAs are mixed in vitro to form RNPs. Next, *C. higginsianum* protoplasts are transformed using donor DNA and CRISPR/Cas9 RNP. Finally, selective media and PCR-based screening techniques are employed to identify strains with the intended HDRs.

The donor DNA for *URA3* knockout was designed to have a *neomycin phosphotransferase II* (*NPTII*) expression cassette conferring G418/geneticin resistance, placed between two homology arms that matched with upstream and downstream regions of the *URA3* coding sequence (CDS; Figure 1b). Two gRNAs were designed to target the CDS of *URA3*. Wild-type *C. higginsianum* protoplasts were transformed using CRISPR/Cas9 RNP and the plasmid-based donor DNA. A negative control was performed with Cas9 but without gRNA. Our result showed that CRISPR/Cas9 RNP increased the number of colonies resistant to G418 approximately fourfold compared to the negative control (Table 1). We then screened the genomic DNA of colonies by PCR to determine the *ura3* mutant rate. We designed two primer sets to amplify two different fragments exclusively present in the genomic DNA from *ura3* mutants that underwent double crossover with the donor DNA (Figure 1b). PCR screening with these primer sets demonstrated that CRISPR/Cas9 RNP greatly increased the HDR rate (Table 1). The *ura3* mutant rate was 98% with gRNA (+gRNA), whereas it was only 3.3% without gRNA (−gRNA). Hence, we successfully generated *ura3* mutants that can be used to establish a marker recycling system.

2.2 | *ura3* mutants show uridine auxotrophy and 5-FOA insensitivity

To confirm the uridine auxotrophy of *ura3* mutants, we assessed the colony diameters of *C. higginsianum* strains cultured on media with or without uridine. As expected, the *ura3* mutants exhibited significantly smaller colony diameters compared to the wild type, while the phenotype was restored upon uridine supplementation, providing

TABLE 1 Number of transformants and the *ura3* mutant rate with or without guide RNAs.

Presence or absence of guide RNA	Number of colonies obtained	Number of colonies tested by PCR	Number of <i>ura3</i> mutants (<i>ura3</i> mutant rate)
−gRNA	30	30	1 (3.3%)
+gRNA	116	50	49 (98%)

Note: “−gRNA” and “+gRNA” represent the results without and with guide RNAs, respectively. The knockout of *URA3* was evaluated by PCR screening as shown in Figure 1c.

evidence of their uridine auxotrophy (Figure 2). To investigate the 5-FOA sensitivity of *C. higginsianum*, we evaluated its impact on colony growth. Fungal *URA3*, in general, is involved in the conversion of 5-FOA to toxic compounds (Boeke et al., 1984; Rossmann et al., 2011). The addition of 5-FOA inhibited the growth of wild-type *C. higginsianum* colonies, indicating their sensitivity to 5-FOA (Figure 2). In contrast, *ura3* mutants were partially resistant to 5-FOA supplementation, thereby confirming the 5-FOA sensitivity of *C. higginsianum* via the *URA3* gene. Therefore, the uridine auxotrophy and the 5-FOA insensitivity of *ura3* mutants indicate the loss of *URA3*-associated enzymatic activities.

2.3 | The *URA3*-based marker recycling system is applicable in *C. higginsianum*

To evaluate the feasibility of using the *URA3* expression cassette as a selection marker in *C. higginsianum*, we aimed to target the *SCD1* gene, which encodes a scytalone dehydratase that is involved in the synthesis of 1,8-DHN-melanin (Kubo et al., 1996). Mutations in *SCD1* are predicted to result in melanin deficiency and scytalone accumulation. By performing a BlastP search using *C. orbiculare* *SCD1* (GenBank ID: TDZ18313.1; Kubo et al., 1996) as a query, we identified a homologue encoded by the *C. higginsianum* genome (locus tag: CH63R_00358). To knock out the *C. higginsianum* *SCD1* gene in the *ura3* mutant background, we employed a combination of the CRISPR/Cas9 system and the donor DNA-mediated HDR. The donor DNA contained a constitutive *URA3* expression cassette (*TEF-URA3*) flanked by homology arms (Figure 3a). We designed two gRNAs to target the *SCD1* CDS. PCR-based screening revealed successful gene knockout of *SCD1*, resulting in strains named *scd1::TEF-URA3 ura3* (Table 2 and Figure 3b). Both the number of colonies and the *scd1::TEF-URA3 ura3* mutant rate increased by introducing CRISPR/Cas9 RNP (Table 2). Our findings suggest that the *TEF-URA3* expression cassette can serve as an effective selection marker in our CRISPR/Cas9 system.

To reuse *TEF-URA3* as a selection marker for sequential gene knockouts, we next aimed to select strains that had lost *TEF-URA3* from the *scd1::TEF-URA3 ura3* strains. As *TEF-URA3* was placed between two identical 500-bp sequences originally derived from the region downstream of the *SCD1* CDS (Figure 3a, blue boxes), strains that lost the cassette via homologous recombination could be selected by incubation on media containing 5-FOA and uridine (Figure 3c). As expected, *scd1::TEF-URA3 ura3* mutants displayed 5-FOA sensitivity (Figure S2), demonstrating that *TEF-URA3* can be effectively used for negative selection on media containing 5-FOA. To isolate *scd1 ura3* mutants, conidia of *scd1::TEF-URA3 ura3* were cultured on medium with 5-FOA and uridine. After several days of incubation, a number of colonies appeared, and genomic DNA PCR analysis revealed the absence of *TEF-URA3* in eight randomly selected colonies. The designated primer amplified 1232-bp fragments in the absence of *TEF-URA3* (Figure 3c), and as expected, the bands were observed from only *scd1 ura3* mutants and not from the

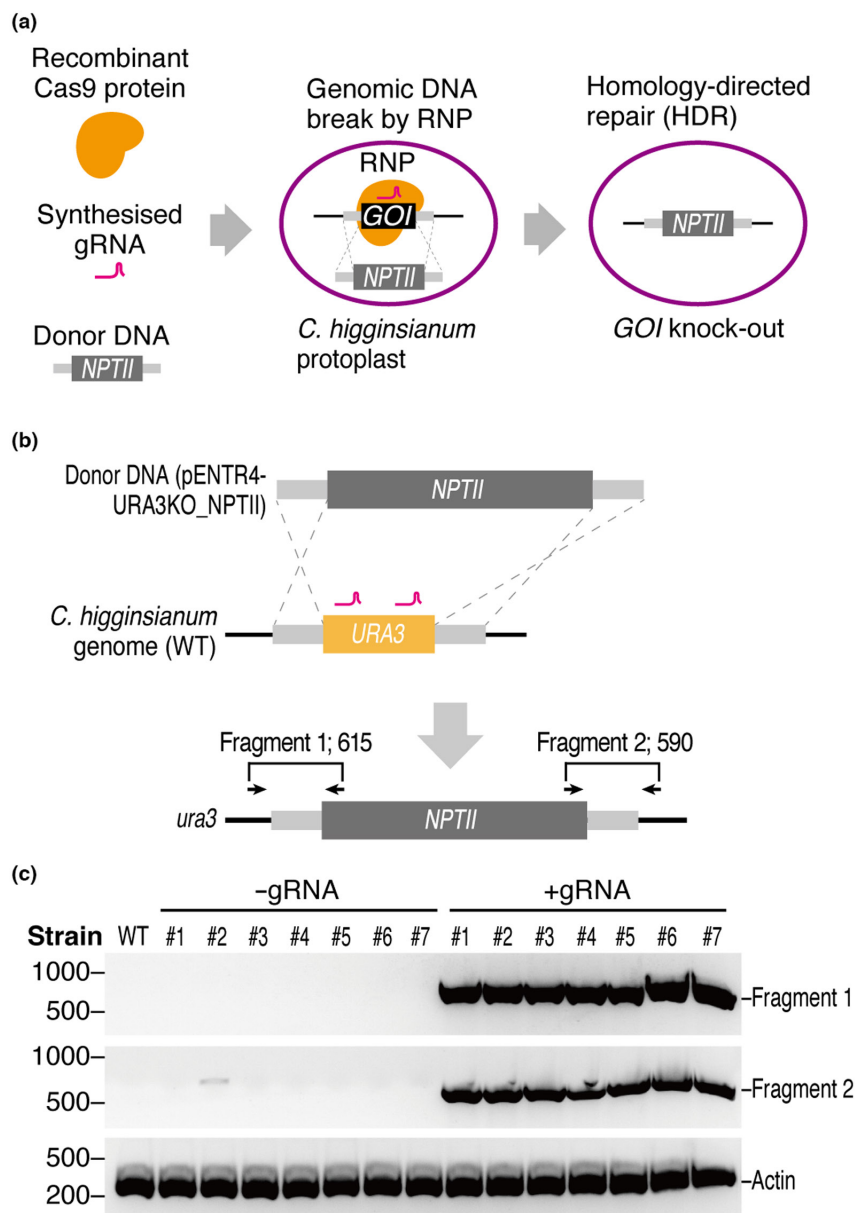


FIGURE 1 CRISPR/Cas9 RNP promotes homologous recombination with donor DNA in *Colletotrichum higginsianum*. (a) Schematics of CRISPR/Cas9 RNP-mediated HDR. Firstly, recombinant Cas9 proteins (in orange) and synthesized gRNAs (in magenta) targeting the gene of interest (*GOI*) were mixed in vitro to form RNPs. Secondly, *C. higginsianum* protoplasts were transformed with RNPs and donor DNAs that have the selection marker, *NPTII*, flanked by two homology arms. Finally, the strain in which the *GOI* was replaced with the selection cassette was isolated by combining growth on selection medium and PCR-based screening. (b) Construction design of *URA3* knockout. The donor DNA has a selection marker, the *NPTII* expression cassette, flanked by 0.5-kb homology arms depicted as light grey boxes. Arrows represent the primers to amplify "Fragment 1" and "Fragment 2" existing specifically in the genome of *ura3*. (c) PCR screening of *ura3* mutants. PCRs were performed using each colony on Mathur's agar containing 500 µg/mL G418 with primer sets depicted in panel (b). Results from seven randomly selected colonies from -gRNA and +gRNA transformants are shown. The 238-bp fragment of the *C. higginsianum* Actin gene (CH63R_04240) was designated as Actin. The numbers on the left of the gels indicate the position of the DNA size marker (bp).

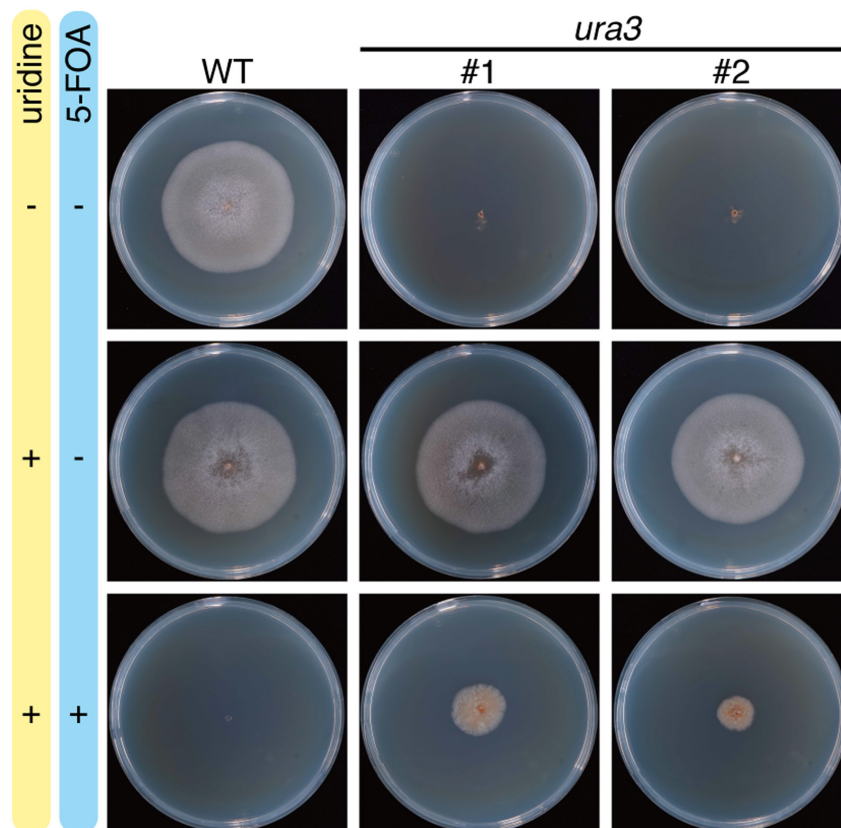
parental strain (Figure 3d). Consistent with the loss of *TEF-URA3*, partial resistance to 5-FOA and uridine auxotrophy of *scd1 ura3* were confirmed (Figure S2). Thus, our results show that the removal of *TEF-URA3* from *scd1::TEF-URA3 ura3* can be achieved through selection after 5-FOA treatment, enabling the reuse of *TEF-URA3* as a selection marker for sequential gene knockouts. These results confirm that the *URA3*-based marker recycling system is applicable in *C. higginsianum*.

2.4 | The *URA3* expression cassette is a reusable selection marker for sequential gene knockout in *C. higginsianum*

To confirm the reusability of *TEF-URA3* as a selection marker for sequential gene knockouts in *C. higginsianum*, we targeted *PKS1* in

scd1 ura3 mutants. *PKS1* encodes a polyketide synthase involved in the production of scytalone in the melanin biosynthesis pathway (Takano et al., 1997; Figure 4a). We identified one *PKS1* homologue in the *C. higginsianum* genome, previously named *ChPKS1* (locus tag: AB508803) and also referred to as *ChPKS19* (locus tag: CH63R_08918; Dallery et al., 2017; Ushimaru et al., 2010), by a BlastP search using *C. orbiculare* *PKS1* (GenBank ID: TDZ26149.1) as the query. *PKS1* was knocked out in *scd1 ura3* using the same method employed for the *SCD1* knockout (Figure 4b). PCR-based screening of 10 randomly obtained colonies resulted in the identification of five colonies that displayed successful knockout of *PKS1*. These strains were named *pkS1::TEF-URA3 scd1 ura3* (Figure 4c). We then selected strains that had lost *TEF-URA3* from the *pkS1::TEF-URA3 scd1 ura3* mutants by culturing them on medium containing 5-FOA and uridine. Using PCR-based screening (Figure 4d), we were able to isolate *pkS1 scd1 ura3* mutants. Thus, our results demonstrate that

FIGURE 2 *ura3* mutants show uridine auxotrophy and 5-fluoroorotic acid (5-FOA) insensitivity. Colonies of wild-type *Colletotrichum higginsianum* and two independent *ura3* mutants on Mathur's agar. Photographs were taken at 7 days postculture. The "+" and "-" symbols indicate the presence and absence of uridine or 5-FOA, respectively. Similar colony growth of each strain on each medium was observed on three independent plates.



the *URA3*-based marker recycling system is applicable to sequential gene knockouts in *C. higginsianum*.

2.5 | *URA3* knock-in complements the uridine auxotrophy of *ura3* mutants

To complement the uridine auxotrophy of *ura3* mutants, we knocked in *C. higginsianum* *URA3* to *ura3* mutants utilizing the CRISPR/Cas9 system. The donor DNA for *URA3* knock-in contained an open reading frame of *URA3* with two homology arms that are homologous to the regions upstream and downstream of the *NPTII* expression cassette (Figure 5a). Two gRNAs targeting the *NPTII* expression cassette were designed and the transformation of *ura3* using the donor DNA and RNPs resulted in the generation of more than 120 colonies. PCR screening of 50 randomly selected colonies revealed that 96% of the colonies (48 colonies) were *URA3* knock-in (KI) strains (*URA3* KI; Figure 5b).

To confirm the complementation of uridine auxotrophy of *URA3* KI, we measured the colony diameters on growth medium. Colonies of *URA3* KIs were as large as those of the wild type (Figure 5c), indicating that the uridine auxotrophy of *ura3* mutants was complemented by *URA3* knock-in. In addition, we assessed the requirement of *URA3* for the pathogenicity of *C. higginsianum* to *A. thaliana*. The inoculation of wild-type *C. higginsianum* caused brownish anthracnose disease symptoms, whereas no symptoms were observed in the *ura3* mutant. The symptomless phenotype of *ura3* was restored

by *URA3* knock-in (Figure 5d), indicating the requirement of *URA3* for the pathogenicity of *C. higginsianum*. Therefore, our results show the successful complementation of uridine auxotrophy and pathogenicity by *URA3* knock-in using the CRISPR/Cas9 system in *C. higginsianum*.

2.6 | *scd1* and *pks1 scd1* show melanin-deficient phenotypes

Given that melanin plays a role in pathogenicity by conferring physical rigidity to appressoria of certain phytopathogenic fungi (Kubo et al., 1991; Ludwig et al., 2014; Woloshuk et al., 1980), we investigated the melanization of *scd1* and *pks1 scd1* mutants. We first complemented the uridine auxotrophy of *scd1 ura3* and *pks1 scd1 ura3* mutants by knocking in the *URA3* gene (Figure S3). Subsequently, we examined the melanization of in vitro appressoria of wild-type *C. higginsianum* and *scd1* and *pks1 scd1* mutants under a microscope. While the appressoria of wild-type *C. higginsianum* were black, those of the *scd1* and *pks1 scd1* mutants were transparent (Figure 6a), indicating a lack of melanin. We then evaluated the pathogenicity of *scd1* and *pks1 scd1* mutants on *A. thaliana* leaves. Notably, no symptoms were observed after inoculation with *scd1* or *pks1 scd1* mutants (Figure 6b), suggesting that melanin is required for the pathogenicity of *C. higginsianum* on *A. thaliana*.

We compared the accumulation of scytalone, a metabolite assumed to be a substrate of SCD1, by exploiting an established

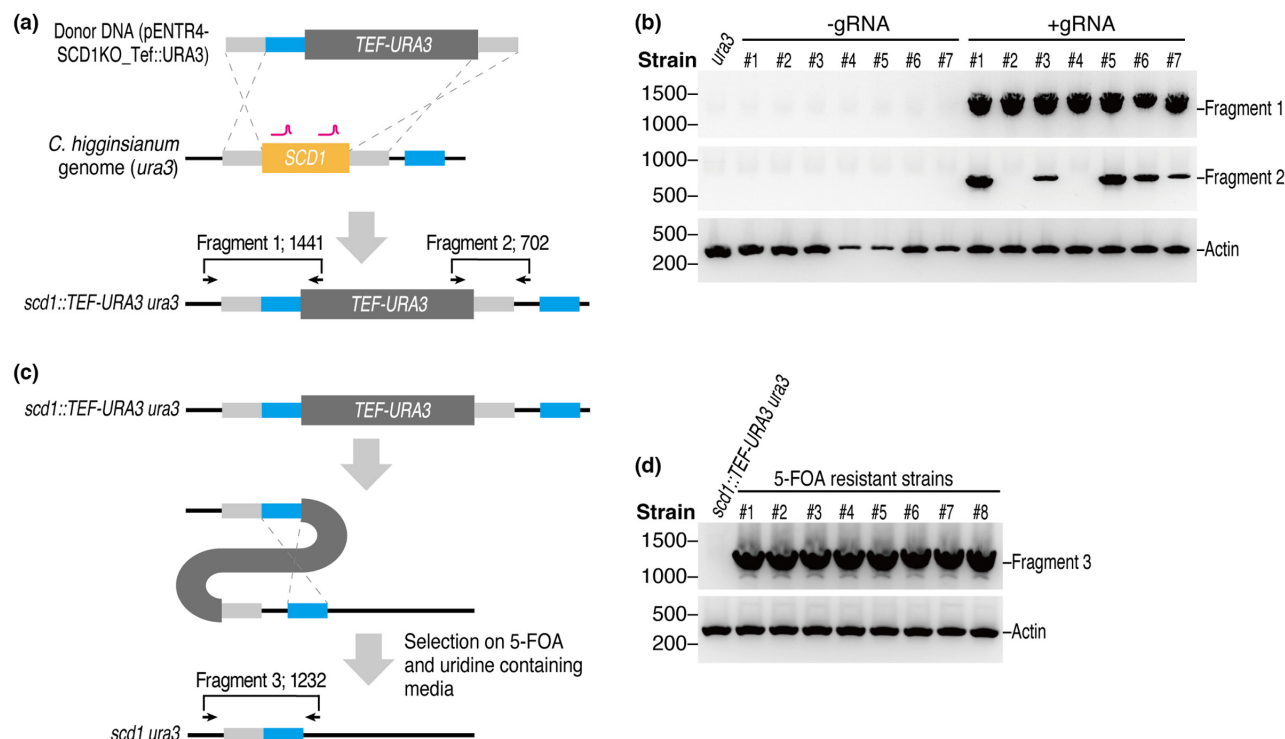


FIGURE 3 *TEF-URA3* is applicable as both positive and negative selection markers. (a) Construction design of *SCD1* knockout in *ura3* mutants. The donor DNA contains *TEF-URA3* flanked by 0.5-kb homology arms depicted as light grey boxes. Lines in magenta represent the sites targeted by gRNAs. Light blue boxes represent homology arms to remove *TEF-URA3* from the genome of *scd1::TEF-URA3 ura3* via homologous recombination as shown in (c). Arrows represent primers to amplify “Fragment 1” and “Fragment 2” existing specifically in the genome of *scd1::TEF-URA3 ura3*. (b) PCR screening of *scd1::TEF-URA3 ura3* mutants. PCRs were performed using primer sets depicted in panel (a). Results from seven randomly selected colonies from –gRNA and +gRNA transformants are shown. (c) Construction design to remove *TEF-URA3* from *scd1::TEF-URA3 ura3* mutants. Arrows represent primers to amplify “Fragment 3” specifically existing in the genome of *scd1 ura3*. (d) PCR screening of *scd1 ura3* mutants. PCRs were performed using each colony grown on Mathur’s medium containing 10mM uridine and 1 mg/mL 5-fluoroorotic acid (5-FOA) with primer sets depicted in (c). Results of eight randomly selected colonies from transformants are shown.

Presence or absence of guide RNA	Number of colonies obtained	Number of colonies tested by PCR	Number of <i>scd1::TEF-URA3 ura3</i> mutants (<i>scd1::TEF-URA3 ura3</i> mutant rate)
–gRNA	16	16	1 (6.3%)
+gRNA	34	32	20 (63%)

Note: “–gRNA” and “+gRNA” represent the results without and with guide RNAs, respectively. The knockout of *SCD1* was evaluated by PCR screening as shown in Figure 3b.

TABLE 2 Number of transformants and the *scd1::TEF-URA3 ura3* mutant rate with or without guide RNAs.

method for in vitro mass production of *C. higginsianum* appressoria (Kleemann et al., 2008). We expected that scytalone would accumulate only in *scd1* but not in wild-type *C. higginsianum* or *pks1 scd1* mutants, because *PKS1* and *SCD1* were assumed to produce a precursor of scytalone and dehydrate scytalone, respectively (Takano et al., 1997). To detect scytalone, we used ultraperformance liquid chromatography (UPLC) coupled with mass spectrometry (MS) to analyse metabolites from in vitro induced *C. higginsianum* appressoria. As expected, scytalone was detected only in *scd1* mutants, but not in wild-type *C. higginsianum* or *pks1 scd1* mutants (Figure 6c). These results support the idea that *PKS1* and *SCD1* play roles in the upstream and downstream steps of scytalone synthesis in the

melanin biosynthesis pathway, respectively (Figure 4a). Moreover, the successful double knockout of *scd1* and *pks1* in the same strain was confirmed by our results.

3 | DISCUSSION

The challenges posed by the low efficiency of gene disruption and the redundancy of virulence factors have hindered the search for virulence factors in many phytopathogenic fungi, including *C. higginsianum* (Collemare et al., 2019; Ushimaru et al., 2010). In this study, we addressed these challenges by introducing two

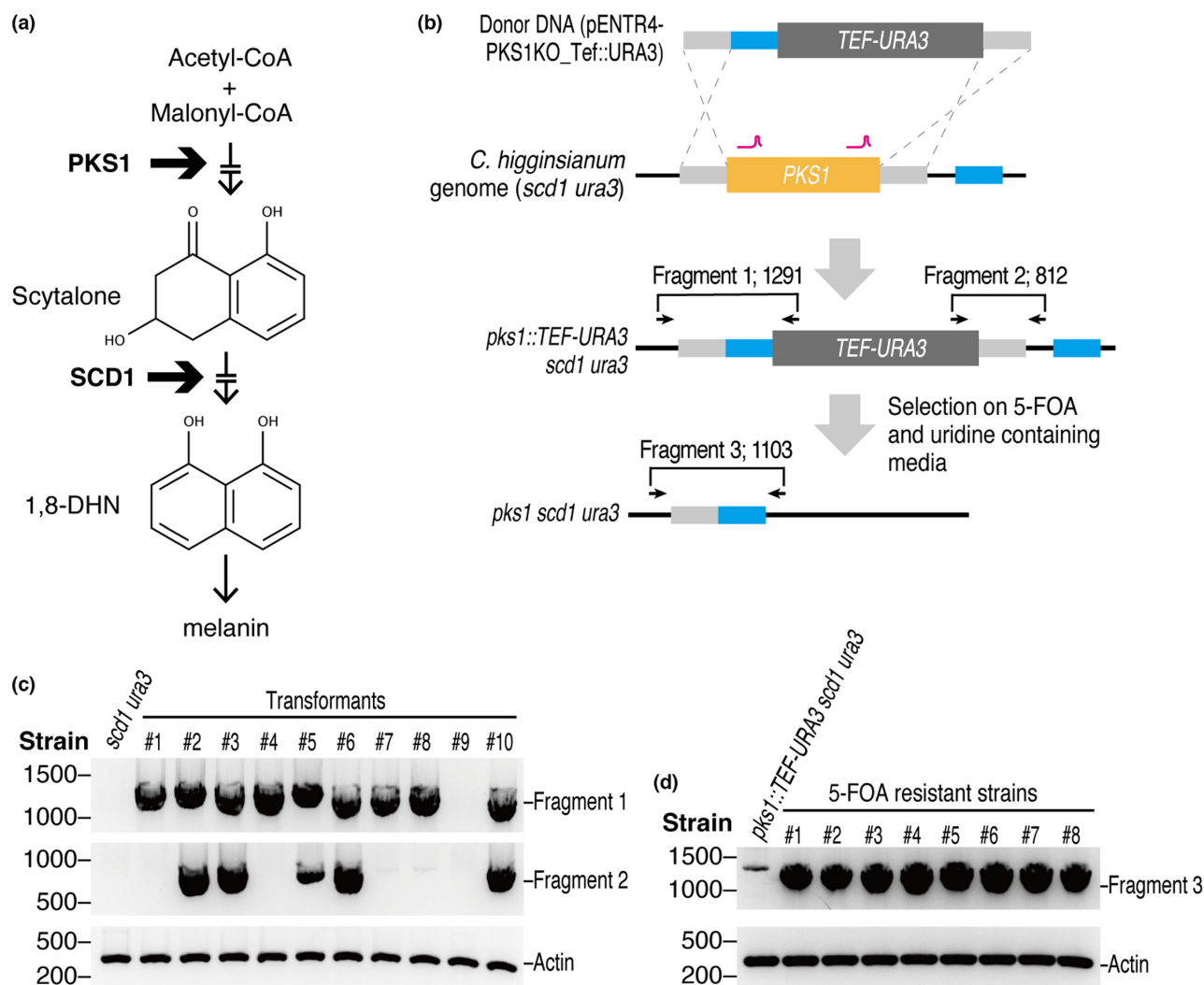


FIGURE 4 The *URA3*-based marker recycling system is applicable for *PKS1* knockout in *scd1 ura3*. (a) Schematic of the assumed melanin biosynthesis pathway in *Colletotrichum higginsianum*. Thin arrows indicate the flow of melanin biosynthesis, and thick arrows indicate the modifications of melanin precursors by *PKS1* or *SCD1*. Gaps inside the arrows indicate that several melanin precursors are omitted for simplification. (b) Construction design of *PKS1* knockout and the removal of *TEF-URA3*. The donor DNA has *TEF-URA3*, flanked by 0.5-kb homology arms depicted as light grey boxes. Lines in magenta represent the sites targeted by gRNAs. Light blue boxes show homology arms to remove *TEF-URA3* from the genome of *pks1::TEF-URA3 scd1 ura3* via homologous recombination. Arrows represent primers used to amplify "Fragment 1" and "Fragment 2" existing specifically in the genome of *pks1::TEF-URA3 scd1 ura3* and "Fragment 3" in the genome of *pks1 scd1 ura3*. (c) PCR screening of *pks1::TEF-URA3 scd1 ura3* mutants. PCRs were performed using the primer sets depicted in panel (b) (Fragments 1 and 2). Results from 10 randomly selected colonies from transformants are shown. (d) PCR screening of *pks1 scd1 ura3* mutants. PCRs were performed using primer sets depicted in panel (b) (Fragment 3). Results from eight randomly selected colonies from transformants are shown.

methods, the CRISPR/Cas9 system and *URA3*-based marker recycling, thereby establishing a highly efficient method for multiple gene disruption in *C. higginsianum*. Our results demonstrated that CRISPR/Cas9 significantly increased the efficiency of gene disruption by donor DNA-mediated homologous recombination. Moreover, we confirmed the feasibility of the *URA3*-based marker recycling approach in *C. higginsianum*, as evidenced by the presence of a single *URA3* homologue and the demonstration of uridine auxotrophy and 5-FOA insensitivity in the *ura3* mutant. Using these methods, we successfully disrupted two melanin biosynthesis genes, *SCD1* and *PKS1*, and confirmed that the sequential knockout

of these genes is possible with high efficiency. Phenotypic analyses revealed that *scd1* and *pks1 scd1* mutants failed to melanize and lost virulence, thereby confirming the effectiveness of our method for analysing virulence factors. Overall, our new method is a significant addition to the toolkit for *C. higginsianum* reverse genetics and will facilitate the future identification of virulence factors, which was previously challenging.

Two methods can be employed for CRISPR/Cas9-based fungal transformation: direct application of in vitro formed RNPs and DNA-mediated expression of RNPs (Schuster & Kahmann, 2019). In this study, we used the in vitro formed RNP approach, which

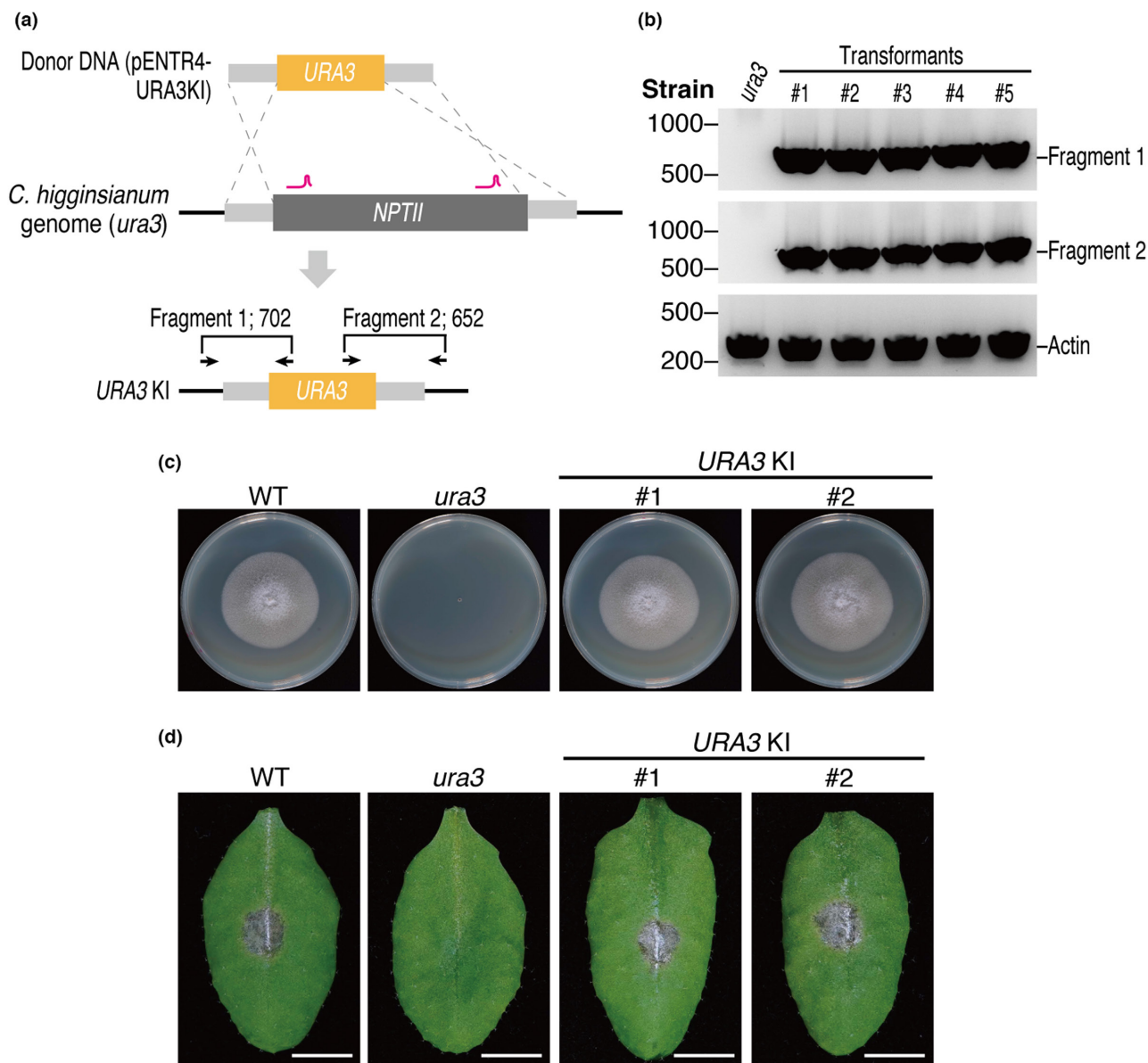
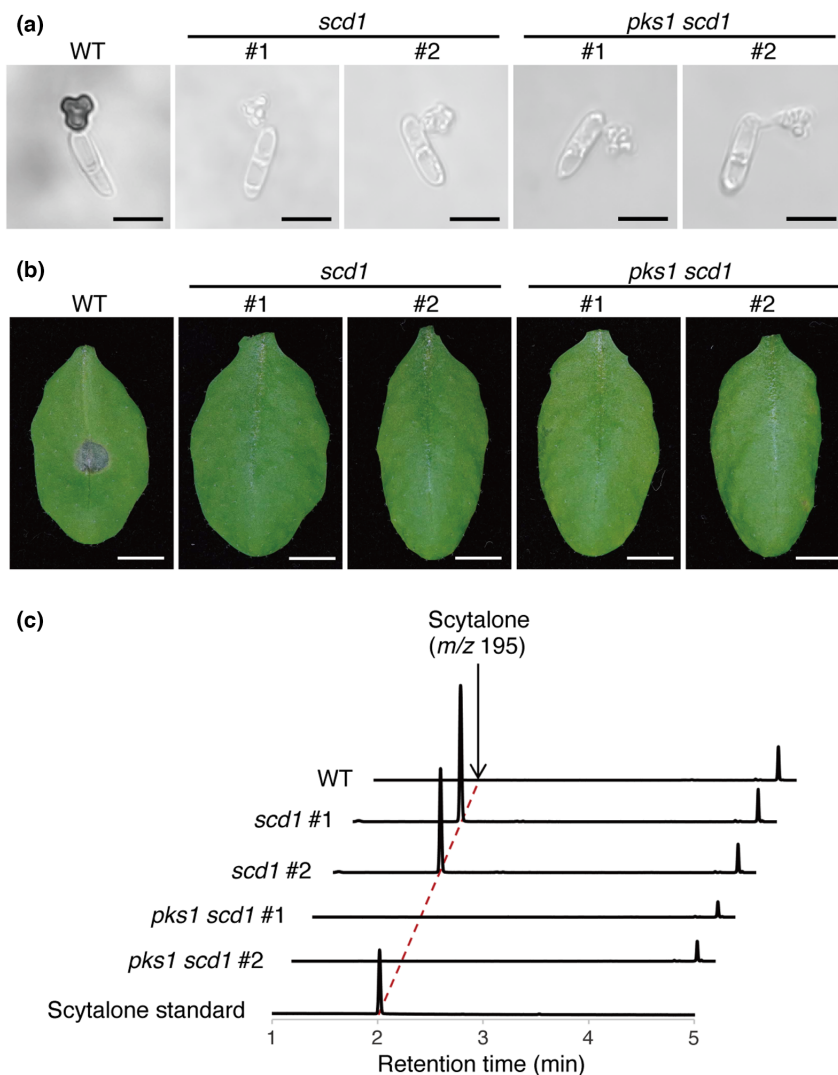


FIGURE 5 *URA3* knock-in (KI) into *ura3* mutants restores uridine auxotrophy. (a) Construction design of *URA3* knock-in into *ura3* mutants. The donor DNA has the *URA3* gene, flanked by 0.5-kb homology arms depicted as light grey boxes. Lines in magenta represent the sites targeted by gRNAs. Arrows represent primers used to amplify "Fragment 1" and "Fragment 2" existing specifically in the genome of *URA3* KI. (b) PCR screening of *URA3* KIs. PCRs were performed using the primer sets depicted in (a). Results from five randomly selected colonies from transformants are shown. (c) Normal colony growth of two independent *URA3* KI strains on Mathur's agar. Photographs were taken at 7 days postculture. Similar colony growth was observed on three independent plates. (d) Disease symptoms on *Arabidopsis thaliana* leaves after inoculation with each genotype of *Colletotrichum higginsianum*. Leaves were observed at 7 days postinoculation. The brownish lesion observed after inoculation with wild-type *C. higginsianum* (WT) and *URA3* KIs was not observed after inoculation with *ura3* mutants ($n=6$). Bars represent 5 mm.

presents two benefits and one drawback. Firstly, the use of in vitro formed RNPs can minimize off-target effects and cytotoxicity as RNPs are present in the cell for a limited time. DNA-mediated expression of RNPs runs the risk of Cas9 and gRNA expression cassettes being integrated into the genome and persistently expressed post-genome editing, leading to off-target effects or cytotoxicity (Foster et al., 2018; Jacobs et al., 2014; Zhang et al., 2015). Secondly, there is no need to scrutinize Cas9 and gRNA expression conditions. Selection of appropriate promoters and codon optimization

are generally necessary for DNA-mediated approaches to induce DSBs (Morio et al., 2020; Nødvig et al., 2015). RNP-based methods do not require these efforts, and determining the required amount of Cas9 and gRNAs for genome editing is straightforward. The disadvantage of the RNP-based approach is its current costliness. DNA-mediated approaches are less expensive than RNP-based approaches using commercially available recombinant Cas9 proteins and synthetic gRNAs because they only require DNA constructs. However, this disadvantage can be remedied by preparing the Cas9

FIGURE 6 Melanin-deficient phenotypes of *scd1* and *pks1 scd1* mutants. (a) Deficiency of melanization in in vitro appressoria of *scd1* and *pks1 scd1* strains compared to the wild type (WT). Appressoria were observed after incubating conidia on glass bottom dishes in a humid box at 25°C for 18–19 h. Bars represent 10 µm. (b) Loss of disease symptoms by *scd1* and *pks1 scd1* inoculation. Leaves were observed at 7 days postinoculation ($n=6$). Bars represent 5 mm. (c) Accumulation of scytalone in appressoria of the *scd1* strain. Metabolites were extracted from in vitro appressorial cells of *Colletotrichum higginsianum* strains and analysed by ultraperformance liquid chromatography coupled with mass spectrometry. Metabolites were detected by measuring absorbance at 281 nm.



protein in-house instead of acquiring it commercially. In our study, a single purification yielded approximately 10 mg of Cas9 protein, more than 100 times the amount necessary for *C. higginsianum* transformation.

The application of CRISPR/Cas9 for improving homologous recombination efficiency offers significant advantages over traditional methods suppressing NHEJ. The conventional approaches that target key NHEJ factors such as *Ku70* or *Lig4* homologues have shown promise in reducing the frequency of NHEJ-mediated DSB repair and thereby increasing the HDR-mediated homologous recombination frequency (Ninomiya et al., 2004; Ushimaru et al., 2010; Zhang et al., 2021). However, this approach has the drawback of disrupting the innate eukaryotic DNA repair mechanism, potentially leading to genome instability and unexpected homologous recombination events (Pastink et al., 2001; Shrivastav et al., 2008). In contrast, the CRISPR/Cas9 method is genetically cleaner, as it does not require the disruption of *Ku70* or *Lig4* homologues. Furthermore, CRISPR/Cas9 can enhance the transformation efficiency by inducing DSBs repaired with donor DNAs. Apart from these advantages, CRISPR/Cas9 has broad applicability beyond homologous recombination.

The CRISPR/Cas9 system can induce mutations without donor DNAs when combined with NHEJ. In *B. cinerea* and *M. oryzae*, CRISPR/Cas9-induced DSBs have been shown to mutate target genes, with NHEJ repairing the break and introducing a deletion or insertion of several bases (Foster et al., 2018; Leisen et al., 2020). Because NHEJ cannot introduce selection markers, unlike donor DNA-mediated homologous recombination, selecting transformants is challenging, in theory. However, in *B. cinerea* and *M. oryzae*, this issue was tackled by co-transforming donor DNA with selection markers along with CRISPR/Cas9 RNPs and isolating them on selective medium, which is called "co-editing." This method's key advantage is that it can simultaneously disrupt multiple genes by using several gRNAs. Nevertheless, the lack of selection markers for each gene requires extensive screening efforts to isolate the desired multiple mutants when the transformation efficiency is not as high as in *B. cinerea*. If transformation efficiency can be further improved in *C. higginsianum*, this method is an attractive technique to apply.

Compared to other marker recycling systems, such as Cre-*loxP* and Flp-FRT, the *URA3*-based system has two notable advantages and one disadvantage. The first advantage is that the *URA3*-based marker recycling process does not leave any foreign sequences

on the genome, whereas the Cre- and Flp-based systems excise DNA between two recombination sites, leaving one site in the recipient genome. In contrast, the integrated foreign sequence can be entirely removed through homologous recombination in the *URA3*-based system, resulting in cleaner knockout lines. The second advantage is its simple donor DNA construction process. Cre-*loxP* requires seven sequences for donor DNA: three gene expression cassettes (positive and negative selection markers and a Cre gene expression cassette), two flanking *loxP* sequences, and two flanking homology arms. In contrast, the *URA3*-based system requires only four sequences: an *URA3* expression cassette and three flanking homology arms, making it easier to construct. However, the *URA3*-based system has the disadvantage, unlike Cre-*loxP* and Flp-FRT, that the parental strain requires an *URA3* mutation. The *URA3* mutation leads to a loss-of-virulence phenotype, which necessitates the knock-in of *URA3* into the *ura3* background when assessing virulence on plants. Nonetheless, this drawback can be overcome by using highly efficient *URA3* knock-in methods such as CRISPR/Cas9, with the *URA3* knock-in rate reaching 96%.

In conclusion, this study presents a highly efficient method for disrupting multiple genes in *C. higginsianum*, including genes that were previously challenging to target. In principle, our method can be applied to fungi capable of transforming protoplasts and carrying *URA3* homologues. Indeed, we have previously used *URA3*-based marker recycling (Kumakura et al., 2019) and CRISPR/Cas9 (Chen et al., 2023) in *C. orbiculare*. The method we developed here has a lower throughput compared to methods reported in organisms that introduce multiple mutations simultaneously by combining RNP-induced DSBs and NHEJ (Leisen et al., 2020; Stuttmann et al., 2021). However, we have demonstrated the potential to combine our in vitro formed RNPs with NHEJ to perform multiple mutageneses simultaneously in *C. higginsianum*. With further improvements in RNP introduction efficiency, this approach can be utilized for easier and faster disruption of multiple target genes.

4 | EXPERIMENTAL PROCEDURES

4.1 | Accession numbers

Accession numbers of *C. higginsianum* genes targeted in this study, *URA3*, *SCD1*, and *PKS1*, are listed in Table S1.

4.2 | Plasmid construction

C. higginsianum genomic DNA used as PCR templates was isolated by the Maxwell RSC Plant DNA Kit with a Maxwell RSC 48 instrument (Promega) following the manufacturer's protocol. PCRs were performed using KOD One PCR Master Mix -Blue- (Toyobo) DNA polymerases. All plasmids used in this study are listed with their contents in Table S2 and Figures S4–S7, and primers to construct plasmids are

listed with their sequences in Table S3. Briefly, fragments for fungal transformation were fused into pENTR4 plasmids (Thermo Fisher Scientific) by HiFi DNA assembly (New England Biolabs). The *NPTII* expression cassette was amplified using the pII99 plasmid (Namiki et al., 2001).

4.3 | CRISPR/Cas9 RNP preparation for transformation

4.3.1 | Cas9 recombinant protein preparation

Cas9 recombinant protein fused with a simian virus 40 nuclear localization signal and a His-tag at the C-terminus (Cas9-NLS-His) was expressed in *Escherichia coli* Rosetta 2 (DE3) cells (Novagen) transformed with pET-Cas9-NLS-6×His (Zuris et al., 2015). Cas9-NLS-His protein expression was induced by overnight incubation at 20°C with isopropyl β-D-1-thiogalactopyranoside at a final concentration of 0.4 mM. The harvested cells were resuspended in immobilized metal chromatography (IMAC) buffer (50 mM Tris-HCl [pH 7.5] and 300 mM NaCl) supplemented with 3 U/μL rLysozyme (Novagen). The cell suspension was sonicated on ice (Ultrasonic disruptor UD-201, TOMY), and the insoluble debris was removed by centrifugation twice (10,000g, 10 min, 4°C). The supernatant was applied to an IMAC column (HisTALON superflow cartridge; Clontech) pre-equilibrated with IMAC buffer. The column was washed with IMAC buffer supplemented with 5 mM imidazole, and the bound protein was eluted with IMAC buffer supplemented with 150 mM imidazole. The eluted fractions containing Cas9-NLS-His were diluted four-fold with 50 mM Tris-HCl (pH 7.5) and subjected to cation exchange chromatography (Hitrap S HP; GE Healthcare) after pre-equilibration with 50 mM Tris-HCl (pH 7.5) and 100 mM NaCl. The bound proteins were eluted in a linear NaCl gradient (100–750 mM). The fractions containing Cas9-NLS-His were pooled and buffer-exchanged into 10 mM Tris-HCl (pH 7.5), 300 mM NaCl, 0.1 mM EDTA, 1 mM dithiothreitol, and 40% glycerol. This Cas9 recombinant protein was stored at –20°C until use.

4.3.2 | gRNA design and preparation

Targeting sequences of gRNAs were determined through the following two steps. Candidate sequences were predicted from the target regions with target cleavage efficiency by the web-based CRISPick software (Doench et al., 2016; Sanson et al., 2018); for each candidate sequence, the likelihood of off-targeting in the *C. higginsianum* genome (GenBank accession: PRJNA47061) was calculated using CasOT (Xiao et al., 2014), and those with lower off-targeting likelihood and higher target cleavage efficiency were selected. Then, gRNAs were synthesized by GenScript or IDT. To enhance the chances of target cleavage, two distinct gRNAs were synthesized for each target gene. Target sequences of gRNA are listed in Table S4.

4.3.3 | CRISPR/Cas9 RNP preparation

First, 100–200 pmol of each gRNA was mixed in a buffer (30 mM HEPES, 100 mM potassium acetate, pH 7.5). The mixture was incubated at 95°C for 3 min and then cooled on ice. Stock solutions of 100 μ M gRNAs were used. To form RNPs in vitro, Cas9 protein (34 μ M in stock) in molar amounts equal to the total molar amount of gRNA was added to the gRNA solution. The mixture was incubated at room temperature for 5 min. Up to 400 pmol of RNPs was mixed with plasmid-based donor DNA for transformation (see Section 4.4.3). The maximum volume of the RNP and donor DNA mixture for a single transformation was 25 μ L.

4.4 | *C. higginsianum* transformation

The parental strain used was *C. higginsianum* (strain ID: IMI349063A; Dallery et al., 2017). All transformation experiments were performed under sterile conditions. The transformation of *C. higginsianum* strains with *URA3* mutations was performed in the same way as that of *C. orbiculare*, as reported in previous reports (Chen et al., 2023; Kumakura et al., 2019) with modifications: *C. higginsianum* strains with *URA3* mutation were cultured on Mathur's agar (MA; 16 mM glucose, 5 mM MgSO_4 , 20 mM KH_2PO_4 , 0.22% [wt/vol] Oxoid mycological peptone, and 3% [wt/vol] agar; Mathur et al., 1950) containing 10 mM uridine (Fujifilm Wako), and 0.6 M glucose minimal medium (1.6 g/L yeast nitrogen base without amino acids [Difco], 4 g/L L-asparagine monohydrate, 1 g/L NH_4NO_3 , 3% [wt/vol] Bacto agar, and 0.6 M glucose, pH 6.0) was used for the selection of the *URA3* CDS-containing transformants. The transformation of *C. higginsianum* strains without *URA3* mutation was performed as follows.

4.4.1 | Conidial preparation

Glycerol stocks of *C. higginsianum* strains stored at -80°C were streaked on MA in 90-mm Petri dishes and incubated at 25°C in the dark. After 7–9 days, pieces of agar with fungal cells were transferred to 100 mL MA in four to five 250-mL flasks by sterile plastic straws. Next, 1 mL sterile water was added to spread fungal cells on the entire surface of the MA plate. Flasks were covered with aluminium foil and sponge plugs for aeration and incubated at 25°C in the dark for 7–10 days.

4.4.2 | Protoplast preparation

Conidia in flasks were suspended in Mathur's liquid medium (16 mM glucose, 5 mM MgSO_4 , 20 mM KH_2PO_4 , and 0.22% [wt/vol] Oxoid mycological peptone; 7.5 mL per flask) and filtered through a cell strainer (100 μ m pore size; Corning). Then, the conidial suspension in 100 mL Mathur's liquid medium (c. 8×10^7 conidia) was incubated in a sterile

300-mL flask for germ tube induction (25°C, 100 rpm, 14–17 h, rotary shaker). Four or five flasks were cultured for each protoplast preparation. Cells were harvested using a cell strainer (100 μ m pore size), washed with 0.7 M NaCl, and resuspended in 20 mL of filter-sterilized (0.2 μ m pore size, Merck) digestion mix (1.2 M MgSO_4 , 10 mM NaPO_4 , and 3% [wt/vol] lysing enzyme from *Trichoderma harzianum* [Merck], pH 5.6). After gently agitating for 3–4 h (60 rpm, 25°C, rotary shaker), the suspension was underlaid with 20 mL of trapping buffer (0.6 M sorbitol, 10 mM Tris-HCl pH 7.5, and 50 mM CaCl_2) and subsequently centrifuged (960 g, 5 min, swinging-bucket rotor). The protoplasts were isolated from the interface between the two layers, rinsed twice with STC (1.2 M sorbitol, 10 mM Tris-HCl pH 7.5, and 50 mM CaCl_2), and resuspended in STC (10^7 – 10^8 protoplasts/mL). Aliquots of 100–150 μ L were stored at -80°C .

4.4.3 | Transformation

Thawed protoplasts were mixed with donor DNA (up to 10 μ g) and CRISPR/Cas9 RNPs (up to 400 pmol) and incubated on ice for 10–20 min. PEG solution (60% [wt/vol] PEG 4000, 10 mM Tris-HCl pH 7.5, and 50 mM CaCl_2) was added in three steps (200, 200, and 800 μ L) with 5 min incubation on ice after each addition. After adding 1 mL STC, protoplasts were mixed with 200 μ L of regeneration medium (0.1% [wt/vol] yeast extract, 0.1% [wt/vol] casein acid hydrolysate [Merck], 1 M sucrose, and 2.4% [wt/vol] Bacto agar) and spread on rectangular plastic Petri dishes (140 \times 100 mm, 40 mL per plate). Dishes were incubated for 6–16 h, overlaid with 20 mL of top medium (3% [wt/vol] Bacto agar) containing 500 μ g/mL G418 (Fujifilm Wako), and incubated at 25°C for 5–7 days. The resulting colonies were transferred to MA containing 500 μ g/mL G418 and incubated for 3–5 days. Transformants were identified as colonies that grew on this second selective medium.

4.5 | Selection of the strains without *TEF-URA3*

TEF-URA3 cassettes were removed from *TEF-URA3*-containing strains basically as previously reported (Kumakura et al., 2019). Briefly, 2 – 5×10^5 conidia were spread on MA containing 1 mg/mL 5-FOA (Fujifilm Wako) and 10 mM uridine and incubated.

4.6 | PCR screening and storage

The genomic DNA of each transformant was isolated following a previously reported method (Liu et al., 2000) and subjected to PCR to confirm the desired transformation. All derivative fungal strains and DNAs used for transformation in this study are listed in Tables S2 and S5, respectively. Primers used for PCR screening are listed in Table S6. Conidia of selected strains were mixed with glycerol at 25% of the final concentration and stored at -80°C for long-term storage.

4.7 | *C. higginsianum* inoculation on *A. thaliana*

Five-week-old leaves of *A. thaliana* Col-0 grown at 22°C under an 8h light/16h dark cycle were used for inoculation. Glycerol stocks of *C. higginsianum* strains stored at -80°C were streaked on MA and incubated at 25°C in the dark. After 7–9 days, pieces of agar with fungal cells were transferred onto 100mL MA in a 250-mL flask, 1 mL sterile water was added, and samples were mixed well. Flasks were covered with aluminium foil and sponge plugs for aeration and incubated at 25°C in the dark. After 7–9 days, conidia were suspended in sterilized water and the concentration was measured by a haemocytometer. Ten microlitres of the conidial suspensions (10^6 conidia/mL) was drop-inoculated onto *A. thaliana* leaves, which were incubated under the same condition as the plant growth in a humid box. After 7 days, the inoculated leaves were detached from plants and photographed.

4.8 | In vitro appressorium preparation

4.8.1 | Conidial preparation

Conidia were prepared as described in the “conidial preparation” section, with a final concentration of 2×10^6 conidia/mL.

4.8.2 | Microscopic observation

The conidial suspension was applied to a 35-mm glass bottom dish (ibidi, IB81218) using a disposable hand-held plastic spray. The inoculated dishes were incubated at 25°C in a humid box for 18–19h. Appressoria were observed and photographed using a BX51 microscope (Olympus) and an LP74 microscope digital camera (Olympus). A UPlanSApo 40x objective lens (Olympus) was used.

4.8.3 | Appressorial lysate

To produce large quantities of in vitro appressoria, a modified version of a previously reported method was used (Kleemann et al., 2008). Briefly, 40mL of conidial suspension in sterile distilled water (2×10^6 conidia/mL) was added to a polystyrene dish (14×10cm) and allowed to settle and adhere to the surface for 40min. A sterile nylon mesh (13×9cm, 50µm pore size) was placed on the surface of the liquid and the excess water was discarded, leaving the nylon mesh to retain water on the dish. After 18–19h incubation at 25°C in a humid box, appressoria that had formed on the bottom of the polystyrene dish were harvested with a cell scraper with 1mL of sterile distilled water. The collected fluid was transferred to 2-mL steel-top tubes and homogenized using 0.6- and 5-mm zirconia beads (BMS) in a bead crusher, ShakeMaster Neo (BMS), at 2000rpm for 2min. The fluid containing crushed appressoria was collected and stored at -80°C for further analysis.

4.9 | Metabolite analysis

Fluid containing crushed appressoria was taken, four volumes of ethanol were added, samples were allowed to settle, and the supernatant was dried under nitrogen. The dried material was dissolved in methanol and analysed by UPLC-MS on an Acquity UPLC H-Class-QDa system (Waters). A reversed-phase column (BEH C18, 2.1×50mm, 1.7µm; Waters) was used at a flow rate of 0.6 mL/min. The mobile phase consisted of water containing 0.1% formic acid (solvent A) and pure acetonitrile (solvent B). The following gradient programme was used: 5% B from 0 to 1min, 5% to 95% B from 1 to 4.5min, 95% B from 4.5 to 5.5min, and re-equilibration with 5% B from 5.5 to 8min. Ultraviolet absorption and positive ion electrospray ionization were used for detection of metabolites. Scytalone was prepared from the cultured broth of carpropamid-treated *Pyricularia oryzae* strain P2 as described previously (Kurahashi et al., 1998).

ACKNOWLEDGEMENTS

This work was supported by a fellowship from the RIKEN Junior Research Associate Program to K.Y., by grants from JSPS (23K05158, JP20K15500, 19KK0397, and JP18K14440) and the Japan Science and Technology Agency (JST; ACT-X, JPMJAX20B4) to N.K., and by grants from JSPS (JP20H05909 and JP22H00364) to K.S. We thank Akiko Ueno, Takuma Aita, Hayato Fukuda, and Reika Hiraishi for their technical assistance.

DATA AVAILABILITY STATEMENT

The data that support the findings of this study are available from the corresponding author upon reasonable request.

ORCID

Katsuma Yonehara  <https://orcid.org/0009-0003-8366-9307>
 Naoyoshi Kumakura  <https://orcid.org/0000-0003-0259-2444>
 Takayuki Motoyama  <https://orcid.org/0000-0001-7602-2394>
 Nobuaki Ishihama  <https://orcid.org/0000-0001-5331-1599>
 Jean-Félix Dallery  <https://orcid.org/0000-0002-0771-9611>
 Richard O'Connell  <https://orcid.org/0000-0002-5358-6143>
 Ken Shirasu  <https://orcid.org/0000-0002-0349-3870>

REFERENCES

- Alani, E., Cao, L. & Kleckner, N. (1987) A method for gene disruption that allows repeated use of *URA3* selection in the construction of multiply disrupted yeast strains. *Genetics*, 116, 541–545.
- Arazoe, T., Miyoshi, K., Yamato, T., Ogawa, T., Ohsato, S., Arie, T. et al. (2015) Tailor-made CRISPR/Cas system for highly efficient targeted gene replacement in the rice blast fungus. *Biotechnology and Bioengineering*, 112, 2543–2549.
- Belhaj, K., Chaparro-Garcia, A., Kamoun, S., Patron, N.J. & Nekrasov, V. (2015) Editing plant genomes with CRISPR/Cas9. *Current Opinion in Biotechnology*, 32, 76–84.
- Birker, D., Heidrich, K., Takahara, H., Narusaka, M., Deslandes, L., Narusaka, Y. et al. (2009) A locus conferring resistance to *Colletotrichum higginsianum* is shared by four geographically distinct *Arabidopsis* accessions. *The Plant Journal*, 60, 602–613.

- Boeke, J.D., Croute, F.L. & Fink, G.R. (1984) A positive selection for mutants lacking orotidine-5'-phosphate decarboxylase activity in yeast: 5-fluoro-orotic acid resistance. *Molecular & General Genetics*, 197, 345–346.
- Cannon, P.F., Damm, U., Johnston, P.R. & Weir, B.S. (2012) *Colletotrichum*—current status and future directions. *Studies in Mycology*, 73, 181–213.
- Capecchi, M.R. (1989) Altering the genome by homologous recombination. *Science*, 244, 1288–1292.
- Chen, M., Kumakura, N., Saito, H., Muller, R., Nishimoto, M., Mito, M. et al. (2023) A parasitic fungus employs mutated eIF4A to survive on roaglate-synthesizing *Aglaia* plants. *eLife*, 12, e81302.
- Clemmensen, S.E., Kromphardt, K.J.K. & Frandsen, R.J.N. (2022) Marker-free CRISPR-Cas9 based genetic engineering of the phytopathogenic fungus, *Penicillium expansum*. *Fungal Genetics and Biology*, 160, 103689.
- Collemare, J., O'Connell, R. & Lebrun, M.-H. (2019) Nonproteinaceous effectors: the terra incognita of plant–fungal interactions. *New Phytologist*, 223, 590–596.
- Dallery, J.-F., Lapalu, N., Zampounis, A., Pigné, S., Luyten, I., Amselem, J. et al. (2017) Gapless genome assembly of *Colletotrichum higginsianum* reveals chromosome structure and association of transposable elements with secondary metabolite gene clusters. *BMC Genomics*, 18, 667.
- Dallery, J.-F., Zimmer, M., Halder, V., Suliman, M., Pigné, S., Le Goff, G. et al. (2020) Inhibition of jasmonate-mediated plant defences by the fungal metabolite higginsianin B. *Journal of Experimental Botany*, 71, 2910–2921.
- Dean, R., Van Kan, J.A., Pretorius, Z.A., Hammond-Kosack, K.E., Di Pietro, A., Spanu, P.D. et al. (2012) The top 10 fungal pathogens in molecular plant pathology. *Molecular Plant Pathology*, 13, 414–430.
- d'Enfert, C. (1996) Selection of multiple disruption events in *Aspergillus fumigatus* using the orotidine-5'-decarboxylase gene, *pyrG*, as a unique transformation marker. *Current Genetics*, 30, 76–82.
- Devkota, S. (2018) The road less traveled: strategies to enhance the frequency of homology-directed repair (HDR) for increased efficiency of CRISPR/Cas-mediated transgenesis. *BMB Reports*, 51, 437–443.
- Doench, J.G., Fusi, N., Sullender, M., Hegde, M., Vaimberg, E.W., Donovan, K.F. et al. (2016) Optimized sgRNA design to maximize activity and minimize off-target effects of CRISPR-Cas9. *Nature Biotechnology*, 34, 184–191.
- Fisher, M.C., Henk, D.A., Briggs, C.J., Brownstein, J.S., Madoff, L.C., McCraw, S.L. et al. (2012) Emerging fungal threats to animal, plant and ecosystem health. *Nature*, 484, 186–194.
- Flynn, P.J. & Reece, R.J. (1999) Activation of transcription by metabolic intermediates of the pyrimidine biosynthetic pathway. *Molecular and Cellular Biology*, 19, 882–888.
- Foster, A.J., Martin-Urdiroz, M., Yan, X., Wright, H.S., Soanes, D.M. & Talbot, N.J. (2018) CRISPR-Cas9 ribonucleoprotein-mediated co-editing and counterselection in the rice blast fungus. *Scientific Reports*, 8, 14355.
- Gratz, S.J., Ukken, F.P., Rubinstein, C.D., Thiede, G., Donohue, L.K., Cummings, A.M. et al. (2014) Highly specific and efficient CRISPR/Cas9-catalyzed homology-directed repair in *Drosophila*. *Genetics*, 196, 961–971.
- Huser, A., Takahara, H., Schmalenbach, W. & O'Connell, R. (2009) Discovery of pathogenicity genes in the crucifer anthracnose fungus *Colletotrichum higginsianum*, using random insertional mutagenesis. *Molecular Plant-Microbe Interactions*, 22, 143–156.
- Jacobs, J.Z., Ciccaglione, K.M., Tournier, V. & Zaratiegui, M. (2014) Implementation of the CRISPR-Cas9 system in fission yeast. *Nature Communications*, 5, 5344.
- Kleemann, J., Rincon-Rivera, L.J., Takahara, H., Neumann, U., van Themaat, E.V.L., van der Does, H.C. et al. (2012) Sequential delivery of host-induced virulence effectors by appressoria and intracellular hyphae of the phytopathogen *Colletotrichum higginsianum*. *PLoS Pathogens*, 8, e1002643.
- Kleemann, J., Takahara, H., Stüber, K. & O'Connell, R. (2008) Identification of soluble secreted proteins from appressoria of *Colletotrichum higginsianum* by analysis of expressed sequence tags. *Microbiology*, 154, 1204–1217.
- Kubo, Y., Nakamura, H., Kobayashi, K., Okuno, T. & Furusawa, I. (1991) Cloning of a melanin biosynthetic gene essential for appressorial penetration of *Colletotrichum lagenarium*. *Molecular Plant-Microbe Interactions*, 4, 440–445.
- Kubo, Y., Takano, Y., Endo, N., Yasuda, N., Tajima, S. & Furusawa, I. (1996) Cloning and structural analysis of the melanin biosynthesis gene *SCD1* encoding scytalone dehydratase in *Colletotrichum lagenarium*. *Applied and Environmental Microbiology*, 62, 4340–4344.
- Kumakura, N., Ueno, A. & Shirasu, K. (2019) Establishment of a selection marker recycling system for sequential transformation of the plant-pathogenic fungus *Colletotrichum orbiculare*. *Molecular Plant Pathology*, 20, 447–459.
- Kurahashi, Y., Araki, Y., Kinbara, T., Pontzen, R. & Yamaguchi, I. (1998) Intermediates accumulation and inhibition sites of Carpropamid in the melanin biosynthesis pathway of *Pyricularia oryzae*. *Journal of Pesticide Science*, 23, 22–28.
- Leisen, T., Bietz, F., Werner, J., Wegner, A., Schaffrath, U., Scheuring, D. et al. (2020) CRISPR/Cas with ribonucleoprotein complexes and transiently selected telomere vectors allows highly efficient marker-free and multiple genome editing in *Botrytis cinerea*. *PLoS Pathogens*, 16, e1008326.
- Liu, D., Coloe, S., Baird, R. & Pederson, J. (2000) Rapid mini-preparation of fungal DNA for PCR. *Journal of Clinical Microbiology*, 38, 471.
- Ludwig, N., Löhner, M., Hempel, M., Mathea, S., Schliebner, I., Menzel, M. et al. (2014) Melanin is not required for turgor generation but enhances cell-wall rigidity in appressoria of the corn pathogen *Colletotrichum graminicola*. *Molecular Plant-Microbe Interactions*, 27, 315–327.
- Mathur, R.S., Barnett, H.L. & Lilly, V.G. (1950) Sporulation of *Colletotrichum lindemuthianum* in culture. *Phytopathology*, 40, 104–114.
- Morio, F., Lombardi, L. & Butler, G. (2020) The CRISPR toolbox in medical mycology: state of the art and perspectives. *PLoS Pathogens*, 16, e1008201.
- Münch, S., Lingner, U., Floss, D.S., Ludwig, N., Sauer, N. & Deising, H.B. (2008) The hemibiotrophic lifestyle of *Colletotrichum* species. *Journal of Plant Physiology*, 165, 41–51.
- Nakamura, M., Okamura, Y. & Iwai, H. (2019) Plasmid-based and -free methods using CRISPR/Cas9 system for replacement of targeted genes in *Colletotrichum sansevieriae*. *Scientific Reports*, 9, 18947.
- Namiki, F., Matsunaga, M., Okuda, M., Inoue, I., Nishi, K., Fujita, Y. et al. (2001) Mutation of an arginine biosynthesis gene causes reduced pathogenicity in *Fusarium oxysporum* f. sp. *melonis*. *Molecular Plant-Microbe Interactions*, 14, 580–584.
- Narusaka, M., Shirasu, K., Noutoshi, Y., Kubo, Y., Shiraishi, T., Iwabuchi, M. et al. (2009) RRS1 and RPS4 provide a dual resistance-gene system against fungal and bacterial pathogens. *The Plant Journal*, 60, 218–226.
- Narusaka, Y., Narusaka, M., Park, P., Kubo, Y., Hirayama, T., Seki, M. et al. (2004) *RCH1*, a locus in *Arabidopsis* that confers resistance to the hemibiotrophic fungal pathogen *Colletotrichum higginsianum*. *Molecular Plant-Microbe Interactions*, 17, 749–762.
- Nielsen, M.L., Albertsen, L., Lettier, G., Nielsen, J.B. & Mortensen, U.H. (2006) Efficient PCR-based gene targeting with a recyclable marker for *Aspergillus nidulans*. *Fungal Genetics and Biology*, 43, 54–64.
- Ninomiya, Y., Suzuki, K., Ishii, C. & Inoue, H. (2004) Highly efficient gene replacements in *Neurospora* strains deficient for nonhomologous end-joining. *Proceedings of the National Academy of Sciences of the United States of America*, 101, 12248–12253.
- Nødvig, C.S., Nielsen, J.B., Kogle, M.E. & Mortensen, U.H. (2015) A CRISPR-Cas9 system for genetic engineering of filamentous fungi. *PLoS One*, 10, e0133085.

- Oakley, B.R., Rinehart, J.E., Mitchell, B.L., Oakley, C.E., Cannona, C., Gray, G.L. et al. (1987) Cloning, mapping and molecular analysis of the *pyrG* (orotidine-5'-phosphate decarboxylase) gene of *Aspergillus nidulans*. *Gene*, 61, 385–399.
- O'Connell, R., Herbert, C., Sreenivasaprasad, S., Khatib, M., Esquerré-Tugayé, M.-T. & Dumas, B. (2004) A novel *Arabidopsis*–*Colletotrichum* pathosystem for the molecular dissection of plant–fungal interactions. *Molecular Plant-Microbe Interactions*, 17, 272–282.
- O'Connell, R.J., Thon, M.R., Hacquard, S., Amyotte, S.G., Kleemann, J., Torres, M.F. et al. (2012) Lifestyle transitions in plant pathogenic *Colletotrichum* fungi deciphered by genome and transcriptome analyses. *Nature Genetics*, 44, 1060–1065.
- Oerke, E.-C. (2006) Crop losses to pests. *Journal of Agricultural Science*, 144, 31–43.
- Pastink, A., Eeken, J.C. & Lohman, P.H. (2001) Genomic integrity and the repair of double-strand DNA breaks. *Mutation Research*, 480–481, 37–50.
- Perfect, S.E., Hughes, H.B., O'Connell, R.J. & Green, J.R. (1999) *Colletotrichum*: a model genus for studies on pathology and fungal-plant interactions. *Fungal Genetics and Biology*, 27, 186–198.
- Rossmann, M.P., Luo, W., Tsaponina, O., Chabes, A. & Stillman, B. (2011) A common telomeric gene silencing assay is affected by nucleotide metabolism. *Molecular Cell*, 42, 127–136.
- Sander, J.D. & Joung, J.K. (2014) CRISPR-Cas systems for editing, regulating and targeting genomes. *Nature Biotechnology*, 32, 347–355.
- Sanson, K.R., Hanna, R.E., Hegde, M., Donovan, K.F., Strand, C., Sullender, M.E. et al. (2018) Optimized libraries for CRISPR-Cas9 genetic screens with multiple modalities. *Nature Communications*, 9, 5416.
- Schuster, M. & Kahmann, R. (2019) CRISPR-Cas9 genome editing approaches in filamentous fungi and oomycetes. *Fungal Genetics and Biology*, 130, 43–53.
- Shrivastav, M., De Haro, L.P. & Nickoloff, J.A. (2008) Regulation of DNA double-strand break repair pathway choice. *Cell Research*, 18, 134–147.
- Stuttman, J., Barthel, K., Martin, P., Ordon, J., Erickson, J.L., Herr, R. et al. (2021) Highly efficient multiplex editing: one-shot generation of 8x *Nicotiana benthamiana* and 12x *Arabidopsis* mutants. *The Plant Journal*, 106, 8–22.
- Takahara, H., Hacquard, S., Kombrink, A., Bledzyn, H.H., Vivek, H., Robin, G.P. et al. (2016) *Colletotrichum higginsianum* extracellular LysM proteins play dual roles in appressorial function and suppression of chitin-triggered plant immunity. *New Phytologist*, 211, 1323–1337.
- Takano, Y., Kubo, Y., Kuroda, I. & Furusawa, I. (1997) Temporal transcriptional pattern of three melanin biosynthesis genes, *PKS1*, *SCD1*, and *THR1*, in Appressorium-differentiating and nondifferentiating conidia of *Colletotrichum lagenarium*. *Applied and Environmental Microbiology*, 63, 351–354.
- Tsushima, A., Gan, P., Kumakura, N., Narusaka, M., Takano, Y., Narusaka, Y. et al. (2019) Genomic plasticity mediated by transposable elements in the plant pathogenic fungus *Colletotrichum higginsianum*. *Genome Biology and Evolution*, 11, 1487–1500.
- Tsushima, A. & Shirasu, K. (2022) Genomic resources of *Colletotrichum* fungi: development and application. *Journal of General Plant Pathology*, 88, 349–357.
- Ushimaru, T., Terada, H., Tsuboi, K., Kogou, Y., Sakaguchi, A., Tsuji, G. et al. (2010) Development of an efficient gene targeting system in *Colletotrichum higginsianum* using a non-homologous end-joining mutant and *Agrobacterium tumefaciens*-mediated gene transfer. *Molecular Genetics and Genomics*, 284, 357–371.
- Weld, R.J., Plummer, K.M., Carpenter, M.A. & Ridgway, H.J. (2006) Approaches to functional genomics in filamentous fungi. *Cell Research*, 16, 31–44.
- Woloshuk, C.P., Sisler, H.D., Tokousbalides, M.C. & Dutky, S.R. (1980) Melanin biosynthesis in *Pyrularia oryzae*: site of tricyclazole inhibition and pathogenicity of melanin-deficient mutants. *Pesticide Biochemistry and Physiology*, 14, 256–264.
- Xiao, A., Cheng, Z., Kong, L., Zhu, Z., Lin, S., Gao, G. et al. (2014) CasOT: a genome-wide Cas9/gRNA off-target searching tool. *Bioinformatics*, 30, 1180–1182.
- Yamada, K., Yamamoto, T., Uwasa, K., Osakabe, K. & Takano, Y. (2023) The establishment of multiple knockout mutants of *Colletotrichum orbiculare* by CRISPR-Cas9 and Cre-loxP systems. *Fungal Genetics and Biology*, 165, 103777.
- Zhang, R., Isozumi, N., Mori, M., Okuta, R., Singkaravanit-Ogawa, S., Imamura, T. et al. (2021) Fungal effector SIB1 of *Colletotrichum orbiculare* has unique structural features and can suppress plant immunity in *Nicotiana benthamiana*. *The Journal of Biological Chemistry*, 297, 101370.
- Zhang, X.-H., Tee, L.Y., Wang, X.-G., Huang, Q.-S. & Yang, S.-H. (2015) Off-target effects in CRISPR/Cas9-mediated genome engineering. *Molecular Therapy. Nucleic Acids*, 4, e264.
- Zuris, J.A., Thompson, D.B., Shu, Y., Guiling, J.P., Bessen, J.L., Hu, J.H. et al. (2015) Cationic lipid-mediated delivery of proteins enables efficient protein-based genome editing *in vitro* and *in vivo*. *Nature Biotechnology*, 33, 73–80.

SUPPORTING INFORMATION

Additional supporting information can be found online in the Supporting Information section at the end of this article.

How to cite this article: Yonehara, K., Kumakura, N., Motoyama, T., Ishihama, N., Dallery, J.-F., O'Connell, R. et al. (2023) Efficient multiple gene knockout in *Colletotrichum higginsianum* via CRISPR/Cas9 ribonucleoprotein and URA3-based marker recycling. *Molecular Plant Pathology*, 00, 1–14. Available from: <https://doi.org/10.1111/mpp.13378>